DESIGN AND EXPERIMENT OF A THRESHING AND SEPARATION SYSTEM FOR A COMB-TYPE WHEAT PLOT HARVESTER BASED ON CFD-DEM

1

基于 CFD-DEM 的梳脱式小麦小区收获机脱分系统设计试验

Wanzhang WANG ¹⁾, Congpeng LI ¹⁾, Xu CHEN ¹⁾, Feng LIU ¹⁾, Shujiang WU ¹⁾, Xindan QIAO ¹⁾, Juxin ZHANG ^{*2)}, Baoshan WANG ^{*1)}

1) College of Mechanical and Electrical Engineering, Henan Agricultural University, Zhengzhou, 450002/ China 2) State Key Laboratory of Intelligent Agricultural Power Equipment, Luoyang, 471039/ China Tel: +86-18739940175; E-mail: wangbs@henau.edu.cn Corresponding author: Baoshan Wang DOI: https://doi.org/10.35633/inmateh-77-63

Keywords: CFD-DEM; Comb-type; Plot harvester; Threshing and separation system; Wheat

ABSTRACT

To address issues such as clogging of threshing units, high grain loss rates, and elevated impurity levels in wheat breeding harvesters, this study developed a combing-type threshing and separation system for wheat plot harvesters. The system adopts a closed plate-tooth threshing drum structure, where the airflow generated by the rotation of drum blades is combined with external impurity-cleaning airflow, thereby reducing material accumulation and seed retention in the threshing and separation system. CFD-DEM coupling simulations determine the optimal parameter combination: when the drum rotational speed is 891 r/min, the feeding rate is 0.58 kg/s, and the impurity-cleaning airflow speed is 22.56 m/s, the system achieves a loss rate of 0.87% and an impurity rate of 9.06%. A field performance test using this parameter combination showed that the system's loss rate was 1.09% and impurity rate was 11.13%. This study provides a reference for the design and research of threshing and separation systems in comb-type wheat plot harvesters.

摘要

为解决小麦育种收获机脱粒装置易堵塞,损失率与含杂率高等问题,本文设计了一种梳脱式小麦小区收获机脱分系统。采用闭式板齿脱粒滚筒结构方案,滚筒叶片旋转产生气流叠加外置清杂气流,有利于减少脱分系统内的物料堆积和存种。CFD-DEM 耦合仿真得出最优参数组合:滚筒转速 891r/min,脱分系统喂入量 0.58kg/s,清杂气流风速 22.56m/s 时脱分系统损失率为 0.87%,含杂率为 9.06%。以此参数组合进行田间性能试验,得到脱分系统损失率为 1.09%,含杂率为 11.13%,试验样机脱分系统达到设计目标,本研究为梳脱式小麦小区收获机脱分系统设计研究提供了参考。

INTRODUCTION

The wheat breeding industry plays a fundamental role in promoting stable agricultural development and ensuring national food security (*Zhu et al., 2015*). Mechanized harvesting for breeding requires a low loss rate, a low impurity rate, and no seed retention (*Shang et al., 2010*). The combination of stringent operational quality requirements, challenging harvesting conditions, and limited mechanized plot harvesting capabilities has created a critical bottleneck in the efficient development of the wheat breeding industry. The threshing and separation system is the core component of plot harvesters. Research into the design and theoretical foundations of threshing and separation systems for wheat plot harvesters is critical for enhancing quality and efficiency of wheat plot harvesting operations (*Fu et al., 2018; Yuan et al., 2024; Yang et al., 2025*).

The international market for breeding harvesters is primarily dominated by WINTERSTEIGER from Austria and HARDRUP from Denmark. Their threshing and separation systems have the functions of threshing and pneumatic seed conveying, with no seed retention during continuous operation. Still, they are large in size, high in power consumption, complex in structure, and expensive (*Yuan et al., 2024*). In recent years, small combine harvesters have been widely used in hilly and mountainous areas, showing good prospects for application in plot breeding harvesting. However, their engine power and cleaning efficiency are low, and the threshing and separation system is prone to blockage, with a high loss rate and impurity rate (*Qu et al., 2024*).

Wanzhang Wang Professor. Ph.D. Eng.; Congpeng Li M.S. Eng.; Xu Chen Ph.D. Eng.; Feng Liu Ph.D. Stud. Eng.; Shujiang Wu M.S. Eng.; Xindan Qiao Ph.D. Stud. Eng.; Juxin Zhang Senior Engineer. M.S. Eng.; Baoshan Wang Lecturer. Ph.D. Eng.

To address this issue, Dai Fei et al. constructed a gas-solid coupling simulation model of the longitudinal axial flow conical threshing device for plot wheat combine harvesters, and the simulation showed that the airflow can make grains and straw move axially, avoiding blockage and seed retention (*Dai et al., 2019*); Yang Ranbing et al. adopted a combined method of a spiral sieve hole cleaning device and a lateral pneumatic auxiliary cleaning system through a compression spring connecting rod self-spring structure, effectively reducing the grain breakage rate and impurity rate (*Yang et al., 2021*). Based on the research of scholars at home and abroad, it is found that relevant scholars mainly study the threshing and separation system of plot breeding harvesters on the basis of traditional wheat combine harvesters. Due to the excessively long straws fed into the threshing and separation system by the traditional header, and the narrow internal space of the plot harvester's threshing device, it is easy to cause blockage of the threshing and separation chamber. The combtype header only feeds the grains, wheat ears, and some short straws removed by the comb stripping drum into the threshing and separation system for re-threshing, which is beneficial to reducing threshing power consumption (*Yuan, et al., 2023*). Therefore, the optimal design of the threshing and separation system for comb-type wheat plot harvesters is of great significance.

In recent years, the CFD-DEM gas-solid coupling numerical simulation method has been widely used to analyze the transportation and separation of particles in the flow field. Liang Zhenwei et al. quantified the air duct resistance by constructing a fluidized grain and sieve airflow resistance model and combined it with CFD simulation to improve cleaning performance (*Liang et al., 2020*). Wu Tao et al. simulated the impurity removal process of the cleaning system using the CFD-DEM method (Wu et al., 2024). Therefore, CFD-DEM gas-solid coupling simulation is an important means to optimize and improve the performance of the threshing and separation system of plot harvesters.

This study addresses the critical challenges of elevated loss rates, elevated impurity rates, and frequent blockage issues in wheat plot breeding harvesters through the development of an innovative threshing and separation system for comb-type wheat plot harvesters. The research employed CFD-DEM coupling simulation combined with field experiments to analyze material motion characteristics within the threshing and separation system, successfully identifying optimal operating parameters for plot harvester operations. These findings establish a foundational framework for future research and development of threshing and separation systems in wheat plot harvesters.

MATERIALS AND METHODS

Design of the Threshing and Separation System

The threshing and separation system is composed of a threshing chamber, a closed-type plate-tooth threshing drum, a concave sieve, an impurity-cleaning and conveying fan, and an auger. The main structure is shown in Fig.1.

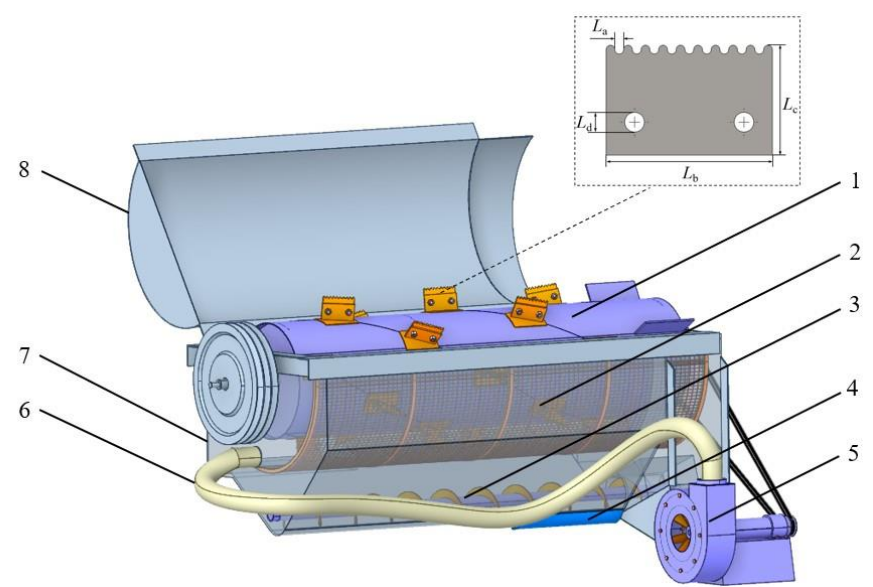


Fig.1 - Main structure of the threshing and separation system

1. Closed-type plate-tooth threshing drum; 2. Concave sieve; 3. Flexible auger;

4. Movable bottom plate of the threshing and separation chamber; 5. Impurity-cleaning fan; 6. Impurity-cleaning air duct; 7. Shell of the threshing and separation chamber; 8. Upper cover plate of the threshing and separation chamber

A closed-type plate-tooth threshing drum is adopted in the threshing and separation system. The impurity-cleaning fan introduces impurity-cleaning airflow through the side plate of the threshing and separation chamber to reduce the accumulation of short straws, wheat ears, and other impurities at the feeding port during operation. Rubber pads are added on the spiral blades of the auger to reduce the conveying gap, and a movable opening is set on the bottom plate of the threshing and separation chamber. The two structural schemes work together to effectively avoid seed retention. During operation, the airflow in the threshing and separation chamber is controlled by changing the rotational speeds of the drum and the impurity-cleaning fan to adjust the impurity-cleaning and conveying effects.

Design of Threshing Drum and Threshing Elements

The closed drum is in a closed state during threshing, which can avoid the entanglement of stems, straws, and other impurities, and has the advantage of low power consumption (*Sudajan et al., 2002*). The design of the threshing drum and threshing elements is shown in Fig. 1.

The plate-tooth shape is designed as a crown plate-tooth with rounded corners to improve threshing capacity and reduce grain damage (Yu et al., 2021). The groove of the threshing plate-tooth should ensure that two seeds pass through at the same time. The average thickness of wheat grains is measured to be 2.91 mm, so the crown plate-tooth groove L_a is set to 6 mm. Referring to the principle of rasp bar threshing, one plate-tooth is arranged with 10 crown teeth to play a kneading role and enhance threshing capacity. The plate-tooth angle not only impacts the wheat ears for threshing but also conveys the threshed materials backward. Appropriately increasing the plate-tooth angle can enhance its ability to convey the threshed materials backward, but more grains will be discharged from the threshing device along with the straws, resulting in a higher loss rate (Wang W., 2007). Therefore, the plate-tooth angle is determined to be 15°, and the height L_c is 50 mm.

Due to the compact structure of the threshing and separation chamber, the cross-sectional length and width are 1100 mm × 440 mm. The threshing gap of wheat is generally 20 mm - 30 mm. Considering the height of the threshing plate-tooth, the inner diameter of the threshing gap drum is 296 mm; the scraper height is set to 60 mm; the axial length of the threshing drum is 1090 mm; to enhance threshing capacity, the plate-teeth at the feeding port are arranged in a staggered manner, with a spacing of 160 mm between two plate-teeth. The threshing plate-teeth are arranged in a 4-head spiral with a pitch of 1600 mm (*Di et al., 2018*). To increase the axial conveying capacity of the drum, the angle between the spiral line and the drum axis is 45°; on the premise of ensuring threshing efficiency, the tooth trace distance is appropriately increased to avoid blockage, and 5 plate-teeth are arranged on each spiral line. When the drum rotates at high speed, the plate-teeth can generate airflow moving axially, promoting the axial conveying of materials between the drum and the concave sieve, and facilitating the threshing and separation processes.

Analysis of Impurity-cleaning Airflow

Impurity-cleaning airflow is an important factor affecting the cleaning performance of the harvester. To avoid material accumulation at the feeding port and blockage, the speed of the impurity-cleaning airflow must be greater than the critical airflow speed at which straws, ear axes, wheat ears, and grains are displaced. However, an excessively high airflow speed will increase the power consumption of the system.

In the process of horizontal material pushing by airflow, the materials in the airflow field are mainly affected by the drag force of the airflow and the maximum static friction force between the materials and the contact surface (*White et al., 2006*). The critical speed equation for materials to start sliding and rolling from rest is as follows:

$$\frac{1}{2}\rho v_y^2 C_d A \ge \mu_s mg \tag{1}$$

Simplified as:

$$v_{y} \ge \sqrt{\frac{2\mu_{s}mg}{\rho C_{d}A}} \tag{2}$$

where:

 ρ - air density, taken as 1.225 kg/m³;

 v_y - critical airflow speed, m/s;

 C_d - drag coefficient;

- A windward area of materials, m²;
- μ_s static friction coefficient between materials and the contact surface;
- *m* mass of materials, kg;
- g gravitational acceleration, taken as 9.8 m/s².

The materials in the threshing and separation system move irregularly, and the windward area changes greatly. Based on the measured three-axis cross-sectional dimensions of the threshing materials, the critical speed at which the threshing materials are displaced under the action of the impurity-cleaning airflow is obtained by equation 2: 5.3-9.2 m/s for wheat grains, 4.8-21.2 m/s for ear axes, 5.1-22.6 m/s for short straws, and 3.8-7.78 m/s for wheat ears. Considering factors such as design errors and changes in conveying conditions, the actual airflow speed should be slightly higher than the theoretically calculated speed. Therefore, the critical speed for the displacement of wheat threshing materials is 5 - 25 m/s.

CFD-DEM Coupling Method and Model Establishment EDEM Model and Parameter Setting

The proportion of mixed materials in the threshing and separation system is determined by bench tests. Mixed materials include 38.2% of grains, 53.2% of wheat ears, and 8.6% of short straws and ear axes. The length of wheat ears ranges from 78.16 mm to 95.03 mm, with an average of 85.51 mm; the length of short straws ranges from 73.06 mm to 144.02 mm, with an average of 102.63 mm.

The wheat grain model is established using a 5-sphere combination model, as shown in Fig. 2A; the ear axis model is simplified as a slender rod formed by a series of small spheres in series, with spherical particles arranged along the length of the ear axis, as shown in Fig. 2B; using Meta-Particle, the position of the grain model on the ear axis is adjusted to establish the discrete element model of the wheat ear, as shown in Fig. 2C; the short straw model is established by particle filling, as shown in Fig. 2D (*Wang et al., 2020*). The simulation parameters of density Poisson's ratio and shear modulus are shown in Table 1 (*Wang et al., 2024*). Coefficients of restitution and friction were obtained through material property tests and calibration tests, informed by references (*Fan et al., 2024; Zhang et al., 2025*), parameters are shown in Table 2.

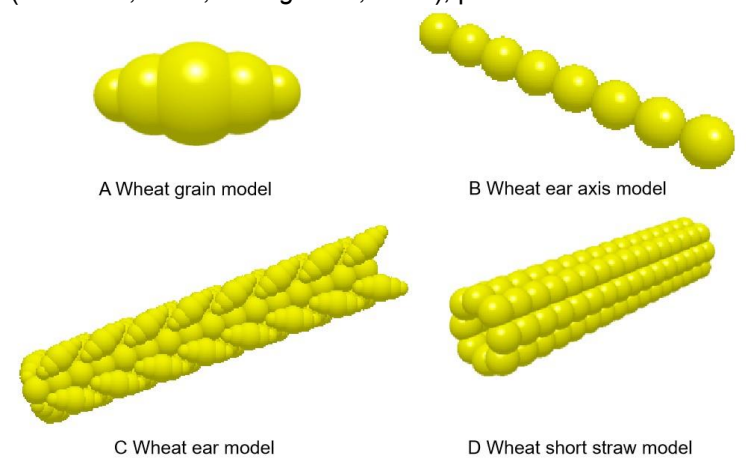


Fig. 2 - Discrete element modeling

Mechanical property parameters of the threshing and separating materials

Materials	Density/(kg⋅m ⁻³)	Poisson's ratio	Shear modulus/(Pa)	
Grain	1350	0.29	4.2×10 ⁶	
Straw	216	0.4	4×10 ⁶	
Ear axis	316	0.4	4×10 ⁶	

Table 2

Materials	Coefficient of Restitution	Coefficient of Static friction	Coefficient of Rolling friction
Grain—Grain	0.46	0.41	0.02
Grain—Steel plate	0.48	0.34	0.01
Grain—Rubber plate	0.32	0.49	0.02
Straw—Grain	0.26	0.33	0.01
Straw—Straw	0.39	0.24	0.01
Straw—Steel plate	0.24	0.32	0.01
Straw—Rubber plate	0.26	0.44	0.01

FLUENT Model Establishment and Mesh Generation

The CFD-DEM coupling simulation model is constructed as follows: 1. The 3D model of the threshing and separation system is simplified using SolidWorks software to improve the speed of mesh model establishment and calculation. 2. The model is saved in .x_t format and imported into SpaceClaim for the extraction of the fluid static region. Rotating dynamic regions are established for the threshing drum, etc. After the fluid static region and rotating dynamic region are established, Inlet, Outlet, and Interface are set. 3. The model is imported into Meshing of Fluent Launcher for surface mesh and volume mesh generation. The curvature adaptive parameters are set, and the mesh quality is evaluated by indicators such as Skewness (<0.6) and Orthogonal Quality (>0.2) for parts with low mesh quality. The simplified model and mesh generation are shown in Fig. 3.

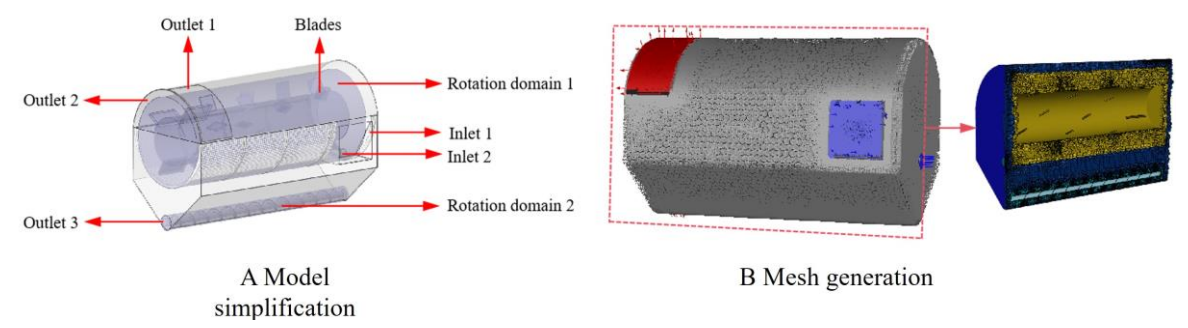


Fig. 3 - Finite element modeling

CFD-DEM Coupling Simulation Method and Design

In Fluent Solution, the gravitational acceleration is along the negative Y-axis, with a value of -9.81 m/s², and the k- ε turbulence model is selected; the air density is 1.225 kg/m³, the dynamic viscosity μ =1.789×10⁻⁵ Pa·s, and the materials in EDEM are inert particles when imported into Fluent, with default working conditions; since the feeding port (Inlet1) of the threshing and separation system has a certain wind force under the action of the comb stripping drum, the wind speed is almost constant due to the attenuation effect of the bridge, so it is set as a velocity inlet (Velocity-Inlet) with a wind speed of 2 m/s, and the direction is perpendicular to the inlet section; the impurity-cleaning airflow inlet (Inlet2) is set as a velocity inlet (Velocity-Inlet); the straw outlet (Outlet1 and Outlet2) and the grain outlet (Outlet3) are set as pressure outlets (Pressure-Outlet), and since they are directly connected to the atmosphere, the gauge pressure P=0 Pa; the time step of the Fluent solver is set to 2×10⁻⁴ s, with a total of 25000 steps; the pre-compiled coupling file is imported and prepared for coupling with EDEM.

In EDEM, according to the proportion of materials fed into the threshing and separation system in the early stage, the generation method is random generation, and the initial feeding speed is 1 m/s; the EDEM time step is set to 1/50 of the Fluent solver time step, the convergence rules for all residuals were set to 1×10^{-4} , and the simulation time is 5 s.

Test Methods

To determine the optimal working parameter combination for threshing and separation performance, the rotational speed of the drum $X_1(800, 900, 1000 \text{ r·min}^{-1})$, the feeding amount of the threshing and separation system $X_2(0.55, 0.60, 0.65 \text{ kg} \cdot \text{s}^{-1})$, and the speed of the impurity-cleaning airflow $X_3(15, 20, 25 \text{ m} \cdot \text{s}^{-1})$ are taken as test factors, and the loss rate and impurity rate are taken as test indicators. The Box-Behnken response surface test with three factors and three levels is set using the central composite rotation design principle. The test factors, levels, test schemes and results are shown in Table 3.

Experiment schemes and results

Table 3

Test	Test factors			Evaluatio	on indicators
No.	Drum rotational speed X ₁	Feeding amount X ₂	Impurity-cleaning airflow speed X ₃	Loss rate Y ₁	Impurity rate Y ₂
1	-1	-1	0	1.40	8.80
2	-1	0	1	0.95	9.40
3	-1	0	-1	1.02	9.67
4	-1	1	0	1.53	9.21
5	0	-1	-1	1.39	9.50
6	0	-1	1	1.40	8.85
7	0	1	-1	2.11	10.04
8	0	0	0	0.91	9.38
9	0	0	0	0.84	9.25
10	0	0	0	0.75	9.39
11	0	1	1	1.53	9.10
12	0	0	0	0.85	9.32
13	0	0	0	0.78	9.21
14	1	0	1	1.73	8.49
15	1	0	-1	1.94	10.20
16	1	-1	0	2.34	8.51
17	1	1	0	2.33	9.16

RESULTS

Analysis of Multi-factor Test Results

The analysis tables of the loss rate and impurity rate of the threshing and separation system are shown in Table 4 and Table 5.

Loss rate analysis

Table 4

Source of variance	Sum of squares	Degrees of freedom	Mean square	F value	<i>P</i> value
<i>X</i> ₁	1.48	1	1.48	111.28	<0.0001**
X_2	0.1176	1	0.1176	8.85	0.0207*
X 3	0.0903	1	0.0903	6.79	0.0205*
X_1X_2	0.0049	1	0.0049	0.3686	0.0351*
X_1X_3	0.0049	1	0.0049	0.3686	0.5629
X_2X_3	0.0870	1	0.087	6.55	0.5629
X_{1}^{2}	0.8087	1	0.8087	60.84	0.0376*
X_{2}^{2}	1.70	1	1.7	128.03	0.0001**
X_{3}^{2}	0.0894	1	0.0894	6.73	0.0357*
Lack of fit	0.0930	7	0.0133		
Residual error	0.0773	3	0.0258	6.56	0.0504
Error	0.0157	4	0.0039		
Total	4.70	16	1		

Note: ** indicates extremely significant influence (P<0.01); * indicates significant influence (0.01≤P<0.05).

Impurity rate analysis

Table 5

Source of variance	Sum of squares	Degrees of freedom	Mean square	F value	<i>P</i> value
<i>X</i> ₁	0.0648	1	0.0648	8.51	0.0224*
X_2	0.4278	1	0.4278	56.16	0.0001**
X 3	1.59	1	1.59	209.13	<0.0001**
X_1X_2	0.0144	1	0.0144	1.89	0.2116
X_1X_3	0.5184	1	0.5184	68.05	<0.0001**
X_2X_3	0.0210	1	0.0210	2.76	0.1406
X_{1}^{2}	0.1095	1	0.1095	14.37	0.4563
X_{2}^{2}	0.2203	1	0.2203	28.92	0.0010**
X_{3}^{2}	0.3572	1	0.3572	46.89	0.0002**
Lack of fit	0.0533	7	0.0076		
Residual error	0.0283	3	0.0094	1.51	0.3406
Error	0.0250	4	0.0062		
Total	3.35	16	/		

Note: ** indicates extremely significant influence (P<0.01); * indicates significant influence (0.01≤P<0.05).

Using Design-Expert 13 software to conduct multiple regression fitting analysis on the test results, and removing the insignificant interaction terms and square terms, the regression equations of the loss rate and impurity rate of the threshing and separation system with each significant factor are obtained as shown in equation 3 and equation 4.

$$Y_{1} = 0.826 + 0.43X_{1} + 0.1213X_{2} - 0.1062X_{3} - 0.035X_{1}X_{2} + 0.4382X_{1}^{2} + 0.6358X_{2}^{2} + 0.1458X_{3}^{2}$$

$$(3)$$

$$Y_2 = 9.31 - 0.09X_1 + 0.2313X_2 - 0.4462X_3 - 0.36X_1X_3 - 0.1613X_1^2 - 0.2288X_2^2 + 0.2912X_3^2$$
 (4)

The analysis of the two significant interaction terms is shown in Fig.4.

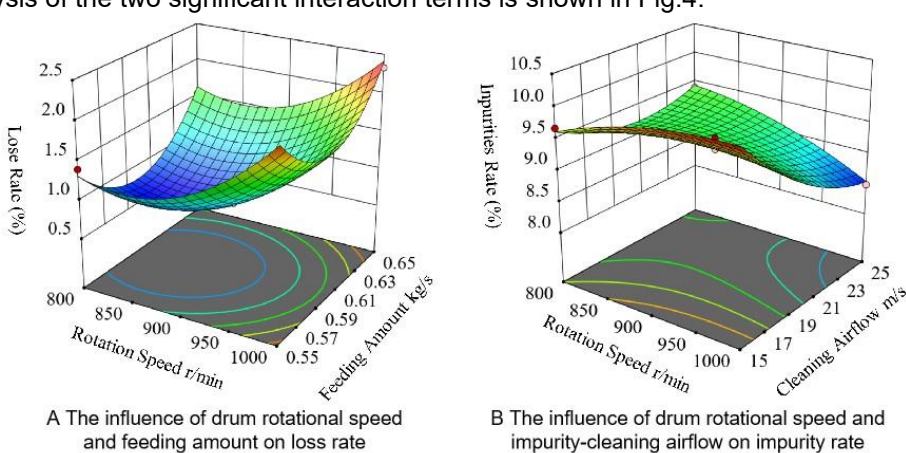


Fig. 4 - Response surface diagram

It can be seen from Fig. 4A that when the feeding amount is constant, the loss rate slightly decreases and then increases with the increase of the threshing drum rotational speed. When the drum rotational speed is greater than about 900 r/min, the loss rate increases rapidly. This is because when the rotational speed is low, the airflow generated is not enough to clear the grains out of the machine, and when the rotational speed reaches about 900 r/min, the threshing is sufficient and the airflow speed is moderate, resulting in the lowest loss rate. As the threshing drum rotational speed continues to increase, the airflow speed increases, and the airflow force can blow both grains and impurities out of the machine, increasing the loss rate.

When the rotational speed of the threshing drum is constant, the loss rate first decreases and then increases with the increase of feeding amount, with an inflection point when the feeding amount increases to 0.57 - 0.60 kg/s; before the inflection point, with the increase of feeding amount, the amount of materials

increases, the resistance between materials increases, the wind force effect decreases, and grains are not easy to be blown out, so the loss rate decreases; after the feeding amount exceeds 0.6 kg/min, the loss rate starts to increase, mainly because the further increase of feeding amount increases the threshing and separation load, thus increasing the loss rate.

It can be seen from Fig. 4B that when the impurity-cleaning airflow speed is less than 20 m/s, the impurity rate changes gently with the increase of drum rotational speed; when the airflow speed is greater than 20 m/s, the impurity rate decreases with the increase of threshing drum rotational speed; when the rotational speed of the threshing drum is low, the impurity rate first decreases and then increases with the increase of impurity-cleaning airflow speed, but the change range is small. When the rotational speed of the threshing drum is 900 - 1000 r/min, the impurity rate gradually decreases, and the change range is significantly larger than that when the rotational speed is 800 - 900 r/min.

Comprehensive response surface analysis shows that the optimal points of loss rate and impurity rate are quite different, and it is necessary to further clarify the optimal working parameter combination of the threshing and separation system.

Optimization of Working Parameters

To determine the optimal working parameters of the threshing and separation system, taking the loss rate Y_1 and impurity rate Y_2 as objectives, combined with the boundary conditions of each test factor, a parameter optimization model is established, as shown in equation 5.

$$\begin{cases} min Y_1 \\ min Y_2 \\ s.t. \begin{cases} 800 < X_1 < 1000 \\ 0.55 < X_2 < 0.65 \\ 15 < X_3 < 25 \end{cases} \end{cases}$$
 (5)

Through optimization calculation, the optimal working parameters are obtained as follows: the rotational speed of the threshing drum is 891 r/min, the feeding amount is 0.58 kg/s, and the impurity-cleaning airflow speed is 22.56 m/s. At this time, the loss rate is 0.87% and the impurity rate is 9.06%.

Field Performance Test

To further verify the accuracy of the simulation test, a field performance verification test was conducted in the Science and Technology Park of Henan Agricultural University, Yuanyang County, Xinxiang City, from June 4 to June 6, 2024. The wheat variety was Weilong 169. The average height of wheat plants was 658 mm, the moisture content was 12-14%, the planting density was 306,800 plants/mu, and the average yield of wheat was 632 kg/mu. An 8×10-meter tarpaulin was prepared and laid on the right side of the harvester to collect the discharged materials. Marking flags were set at the start and end of the test, with a working distance of 10 meters. The field test was conducted with the optimal working parameters obtained from the previous simulation. The drum rotational speed and airflow speed were controlled by changing the gear of the harvester and the size of the pulley, and monitored by a Sanliang TM690 tachometer and a Sima AS8336 anemometer. The feeding amount was controlled by the forward speed.

The field performance test is shown in Fig. 5, and the results of the loss rate and impurity rate of the threshing and separation system are shown in Table 6.



Fig. 5 - Field performance test

Field results of threshing and separating performance

Table 6

Index No.	Loss rate (%)	Impurity rate (%)
1	1.07	9.60
2	0.95	12.32
3	1.41	13.69
4	1.24	8.57
5	0.78	11.47
Average	1.09	11.13

The field performance test showed that the threshing and separation system of the comb-type wheat plot combine harvester had no blockage during operation, no material residue on the concave sieve after operation, and no seed retention on the bottom plate of the threshing and separation chamber. Quantitative performance analysis revealed an average loss rate of 1.09% and an impurity rate of 11.13%. The test showed that the cleaning and threshing performance of the threshing and separation system of the comb-type plot harvester was good, meeting the design requirements.

CONCLUSIONS

- (1) This study presents the development of the threshing and separation system's operational principles and optimized design of critical components. The system incorporates strategically positioned impurity-cleaning and conveying airflow mechanisms that effectively transport and clean accumulated materials from the concave sieve base. This integrated approach resolves blockage and seed retention challenges within the threshing and separation system while simultaneously reducing loss rates and impurity rates.
- (2) This research employed a CFD-DEM gas-solid coupling model to simulate the threshing and separation system and analyze material accumulation patterns across various airflow configurations. Taking the rotational speed of the threshing drum, feeding amount, and impurity-cleaning and conveying airflow speed as factors, and the loss rate and impurity rate as evaluation indicators, multi-factor tests are conducted through coupling simulation, and regression models between the loss rate, impurity rate, and each significant factor are established. The optimal working parameters of the threshing and separation system are determined, and the results show that when the rotational speed of the threshing drum of 891 r/min, the feeding amount of 0.58 kg/s, and the impurity-cleaning airflow speed of 22.56 m/s, the loss rate of 0.87% and the impurity rate of 9.06%.
- (3) Field performance testing was conducted to verify effectiveness of the threshing and separation system under optimal operating parameters. The results demonstrated exceptional system reliability, with no blockage or material residue observed on the concave sieve, and complete elimination of seed retention on the threshing and separation chamber base plate. Performance metrics revealed an average loss rate of 1.09% and an impurity rate of 11.13% for the threshing and separation system. These results confirm that the comb-type wheat plot harvester's threshing and separation system satisfy all design specifications and performance requirements.

ACKNOWLEDGEMENTS

This work was financially supported by China Agriculture Research System (CARS-03)and State key laboratory of intelligent agricultural power equipment open project "Hydraulic control system design of hydraulic drive track-laying vehicle" (SKLIAPE 2024011).

REFERENCES

- [1] Dai, F., Song, X., Zhao, W., Han, Z., Zhang, F., & Zhang, S. (2019). Motion simulation and test on threshed grains in tapered threshing and transmission device for plot wheat breeding based on CFD-DEM. *International Journal of Agricultural and Biological Engineering*, 12(1), 66-73. USA.
- [2] Di, Z., Cui, Z., Zhang, H., Zhou, J., Zhang, M., & Bu, L. (2018). Design and experiment of rasp bar and nail tooth combined axial flow corn threshing cylinder (纹杆块与钉齿组合式轴流玉米脱粒滚筒的设计与试验). *Transactions of the Chinese Society of Agricultural Engineering*, 34(1), 28-34. Beijing/China.
- [3] Fan, J., Wang, H., Sun, K., Zhang, L., Wang, L., Zhao, J., & Yu, J. (2024). Experimental verification and simulation analysis of a multi-sphere modelling approach for wheat seed particles based on the discrete element method. *Biosystems Engineering*, 245, 135-151. UK.

- [4] Fu, J., Chen, Z., Han, L., & Ren, L. (2018). Review of grain threshing theory and technology. *International Journal of Agricultural and Biological Engineering*, 11(3), 12-20. USA.
- [5] Hussain, S., Zheng, D., Song, H., Farid, M. U., Ghafoor, A., Ba, X., Wang, H., Wang, W., Sher, A., & Alshamali, S. J. (2022). Computational fluid dynamics simulation and optimisation of the threshing unit of buckwheat thresher for effective cleaning of the cleaning chamber. *Journal of Agricultural Engineering*, 53(1). Italy.
- [6] Liang, Z., Xu, L., De Baerdemaeker, J., Li, Y., & Saeys, W. (2020). Optimisation of a multi-duct cleaning device for rice combine harvesters utilizing CFD and experiments. *Biosystems Engineering*, 190, 25-40.
- [7] Qu, Z., Lu, Q., Shao, H., Le, J., Wang, X., Zhao, H., & Wang, W. (2024). Design and test of a grain cleaning loss monitoring device for wheat combine harvester. *Agriculture*, 14(5), 671. Switzerland.
- [8] Shang, S., Yin, Y., Guo, P., & Sun, Q. (2010). Current situation and development trend of mechanization of field experiments (国际田间试验机械的发展现状及展望). *Transactions of the Chinese Society of Agricultural Engineering*, 26(1), 5-8. Beijing/China.
- [9] Sudajan, S., Salokhe, V. M., & Triratanasirichai, K. (2002). PM-Power and machinery: effect of type of drum, drum speed and feed rate on sunflower threshing. *Biosystems engineering*, *83*(4), 413-421. UK.
- [10] Wang, Q., Mao, H., & Li, Q. (2020). Modelling and simulation of the grain threshing process based on the discrete element method. *Computers and Electronics in Agriculture*, 178, 105790. Netherlands.
- [11] Wang, W. (Ed.). (2007). Agricultural machinery design handbook. *China Agricultural Science and Technology Press*. Beijing/China.
- [12] Wang, W., Wu, S., & Li, C. (2024). Design and experiment of single ear electric thresher for wheat breeding (小麦育种单穗电动脱粒机设计与试验) [J]. *Journal of Henan Agricultural University*, *58*(2), 259-268. Zhengzhou/China.
- [13] White, F. M., & Majdalani, J. (2006). Viscous fluid flow (Vol. 3, pp. 433-434). New York: McGraw-Hill. Wu, T., Li, F., Liu, Q., Ren, J., Huang, J., & Qin, Z. (2024). Numerical Simulation and Analysis of the Impurity Removal Process of a Sugarcane Chopper Harvester Based on a CFD–DEM Model. *Agriculture*, 14(8), 1392. Switzerland.
- [14] Wu, T., Li, F., Liu, Q., Ren, J., Huang, J., & Qin, Z. (2024). Numerical Simulation and Analysis of the Impurity Removal Process of a Sugarcane Chopper Harvester Based on a CFD–DEM Model. *Agriculture*, 14(8), 1392. Switzerland.
- [15] Yang, R., Chen, D., Zha, X., Pan, Z., & Shang, S. (2021). Optimization design and experiment of earpicking and threshing devices of corn plot kernel harvester. *Agriculture*, 11(9), 904. Switzerland.
- [16] Yang, R., Wang, P., Qing, Y., Chen, D., Chen, L., & Sun, W. (2025). Discrete element simulation optimization design and testing of low-damage flexible drum threshing elements suitable for high-quality seed harvesting. *Scientific Reports*, 15(1), 13601. UK.
- [17] Yu, Y., Li, L., Zhao, J., Wang, X., & Fu, J. (2021). Optimal design and simulation analysis of spike tooth threshing component based on DEM. *Processes*, 9(7), 1163. Switzerland.
- [18] Yuan, L., He, X., Zhu, C., Wang, W., Wang, M., & Wu, S. (2024). Design and test of tangential and longitudinal-axial threshing and separating unit for wheat. *Results in Engineering*, 21, 101774. Netherlands.
- [19] Yuan, L., Lan, M., He, X., Wei, W., Wang, W., & Qu, Z. (2023). Design and experiments of a double-cutterbar combine header used in wheat combine harvesters. *Agriculture*, 13(4), 817. Switzerland.
- [20] Yuan, X., Huang, C., Tao, G., Yi, S., & Li, Y. (2024). Design and Experiment of Oil-Electric Hybrid Air-Suction Sorghum Plot Seeder. *Agriculture*, 14(3), 432. Switzerland.
- [21] Zhang, X., Tao, G., Xu, Y., & Yu, C. (2025) Construction and parameter calibration of a discrete element model of barley seedling stems. *INMATEH Agricultural Engineering*, 77(3), 30-43. Romania.
- [22] Zhu, M., Chen, H., & Li, Y. (2015). Investigation and development analysis of seed industry mechanization in China (中国种业机械化现状调研与发展分析). *Transactions of the Chinese Society of Agricultural Engineering*, 31(14), 1-7. Beijing/China.